



This is a repository copy of *Monolithically integrated μ LEDs/HEMTs microdisplay on a single chip by a direct epitaxial approach*.

White Rose Research Online URL for this paper:
<https://eprints.whiterose.ac.uk/173699/>

Version: Published Version

Article:

Cai, Y., Zhu, C., Zhong, W. et al. (3 more authors) (2021) Monolithically integrated μ LEDs/HEMTs microdisplay on a single chip by a direct epitaxial approach. *Advanced Materials Technologies*, 6 (6). 2100214. ISSN 2365-709X

<https://doi.org/10.1002/admt.202100214>

Reuse

This article is distributed under the terms of the Creative Commons Attribution (CC BY) licence. This licence allows you to distribute, remix, tweak, and build upon the work, even commercially, as long as you credit the authors for the original work. More information and the full terms of the licence here:
<https://creativecommons.org/licenses/>

Takedown

If you consider content in White Rose Research Online to be in breach of UK law, please notify us by emailing eprints@whiterose.ac.uk including the URL of the record and the reason for the withdrawal request.



eprints@whiterose.ac.uk
<https://eprints.whiterose.ac.uk/>

Monolithically Integrated μ LEDs/HEMTs Microdisplay on a Single Chip by a Direct Epitaxial Approach

Yuefei Cai, Chenqi Zhu, Wei Zhong, Peng Feng, Sheng Jiang, and Tao Wang*

There is a significantly increasing demand on developing a microLED (μ LED) based microdisplay which may be the only display system that can meet the requirements for augmented reality/virtual reality systems, helmet mounted displays, and head-up displays. However, a number of fundamental challenges which cannot be met by any existing technologies need to be overcome before such a microdisplay with satisfied performance becomes possible. In this paper, a different type of integration concept using an epitaxial approach is proposed, aiming to monolithically integrate μ LEDs and high electron mobility transistors (HEMTs) on a single chip. This concept can be potentially realized by using a selective epitaxial overgrowth method on a predefined HEMT template featuring microhole masks. Finally, the proposed epitaxial integration concept is translated into a prototype, demonstrating an 8×8 microLED microdisplay, where each μ LED is electrically driven by an individual HEMT which surrounds its respective μ LED via the gate bias of the HEMT.

III-nitride LEDs exhibit a few orders of magnitude higher illuminance^[1–3] and 1–2 orders of magnitude higher ACR than OLEDs.^[1,2] Furthermore, OLEDs have to be heavily driven using high injection current to obtain brightness which has to be several times higher than that required due to the utilization of a color filter.^[3] Therefore, a microLED microdisplay represents the best option.^[4–12]

Basically, a microLED microdisplay mainly consists of μ LED arrays and electronic parts which electrically drive individual μ LEDs. Currently, two main approaches are used to integrate μ LED arrays and electronic parts. The first approach is so-called “pick-and-place” which is based on a massive transfer technology, meaning that millions of μ LEDs

are transferred from a wafer to a transistor backplane, where a very high accuracy of around $1 \mu\text{m}$ and a considerable amount of time are required. As a result, the yield is generally very low,^[13–16] and thus this approach is impractical for manufacturing a microdisplay, especially for AR/VR applications. The second approach is based on a flip-chip bonding technology, where μ LEDs and a CMOS (which is used to electrically drive individual μ LEDs) are fabricated separately and are then heterogeneously wafer-bonded together.^[17] However, it is worth highlighting that the second approach is facing two major challenges. The first challenge is due to an assembly issue. Since individually addressable μ LEDs need to be driven by CMOS circuits, a heterogeneous integration method is adopted to combine μ LEDs with electrically driving parts.^[4,8–13] In this case, there still exists an accuracy issue of the alignment between μ LEDs and CMOS, thus still limiting a transfer yield and then increasing manufacturing costs. The second challenge is due to a degradation in the optical performance of μ LEDs, where μ LEDs are fabricated by means of a photolithography technique and subsequent dry-etching processes.^[4–11] During such dry-etching and follow-up processes, severe damages are introduced, leading to a severe degradation in the optical performance of μ LEDs.^[18,19] Moreover, with scaling down the size of μ LEDs, the severity of the issue is further enhanced.^[18–22] Although an extra passivation process using an atomic layer deposition (ALD) technique is adopted,^[22,23] the recovery of optical performance is marginal due to irreversible damages caused during dry-etching processes. Therefore, such a heterogeneous integration approach for the fabrication of a microdisplay is still far from satisfactory.


We believe that an epitaxial integration of μ LEDs and high electron mobility transistors (HEMTs) that electrically drive

1. Introduction

A microdisplay, which is defined as an ultrasmall screen with <1 in. in diagonal, is the key element for a wide range of next-generation display systems, such as augmented reality (AR)/virtual reality (VR) systems, helmet mounted displays (HMD), and head-up displays (HUD), which are typically used in small spaces or at close proximity to the eye. As a result, high resolution, high luminance (to achieve sufficient ambient contrast ratio (ACR)), and a small form factor are required. However, current liquid crystal on silicon or digital light processor based projection microdisplay cannot meet these requirements due to their intrinsic limitations.^[1–3] In contrast, it is expected that a microdisplay based on III-nitride inorganic semiconductor microLED (μ LED) technologies has a great potential to eliminate these limitations.

Compared with an organic LED (OLED), an inorganic microLED has the potential to provide high luminance without concerning about reliability and lifetime issues.^[2,4] In general,

Dr. Y. Cai, C. Zhu, W. Zhong, P. Feng, Dr. S. Jiang, Prof. T. Wang
Department of Electronic and Electrical Engineering
The University of Sheffield
Mappin Street, Sheffield S1 3JD, UK
E-mail: t.wang@sheffield.ac.uk

 The ORCID identification number(s) for the author(s) of this article can be found under <https://doi.org/10.1002/admt.202100214>.

© 2021 The Authors. Advanced Materials Technologies published by Wiley-VCH GmbH. This is an open access article under the terms of the Creative Commons Attribution License, which permits use, distribution and reproduction in any medium, provided the original work is properly cited.

DOI: 10.1002/admt.202100214

individual μ LEDs might be the ultimate approach to the fabrication of a microdisplay. Very recently, we have developed an epitaxial growth approach to the formation of μ LEDs on a prepatterned template, namely, the formation of μ LEDs does not involve any dry-etching processes, thus eliminating any resultant etching damages.^[24–26] As a result, we have demonstrated ultrasmall μ LEDs with a record external quantum efficiency (EQE).^[24,25] In this paper, we propose a concept, namely, a prepatterned HEMT structure instead of a single GaN template is used as a template, on which μ LEDs will be subsequently grown. This aims to achieve an epitaxial integration of μ LEDs and HEMTs for a microdisplay, where we expect that all the fundamental issues which cannot be overcome in either “pick-and-place” or “flip-chip bonding technology” can be eliminated. In this paper, we have translated the proposed epitaxial integration concept into a prototype, demonstrating an 8×8 microLED microdisplay, where each μ LED is electrically driven by an individual HEMT.

2. Experimental Section

Figure 1a shows a 3D layout for our 8×8 μ LED microdisplay. Figure 1b illustrates the schematic of the cross section of a single μ LED as a pixel, demonstrating each μ LED which is selectively overgrown on a prepatterned HEMT template can be electrically driven by the circular gate of each HEMT surrounding a μ LED, namely, all μ LEDs are individually addressable via HEMTs.

In our previous work (i.e., not individually addressable μ LEDs), a single n-GaN layer on sapphire was used as a template for the selective overgrowth of μ LED arrays.^[24,25] In this work, an AlGaIn/GaN HEMT structure instead of a single n-GaN layer is used as a template to achieve a microdisplay via an epitaxial integration of μ LEDs and HEMTs, where each μ LED is individually driven by a HEMT. The HEMT template consists of a 25 nm $\text{Al}_{0.20}\text{Ga}_{0.80}\text{N}$ barrier and a 1 nm AlN spacer in addition to a 1 μm GaN buffer layer and a high temperature AlN buffer layer which is directly grown on *c*-plane sapphire.

Using our high temperature AlN buffer approach, our HEMTs have demonstrated an extremely high breakdown field and an extremely low leakage current.^[27] Such a HEMT structure can electrically drive individual μ LEDs without concerning about leakage current which may unintentionally turn on μ LEDs which are supposed to be off. For the details of our HEMT structure, please refer to our paper recently published elsewhere.^[27]

Subsequently, a SiO_2 film with a thickness of 500 nm is deposited on the HEMT template by using a plasma-enhanced chemical vapor deposition (PECVD) technique. A photolithography technique and then drying etching processes are used to selectively etch the SiO_2 mask down to the surface of the HEMT template, forming regularly arrayed microholes with a diameter of 20 μm . Next, a standard InGaIn-based LED structure is selectively overgrown on the patterned template. The LED structure consists of a n-type GaN layer, an $\text{In}_{0.05}\text{Ga}_{0.95}\text{N}$ prelayer, five-period InGaIn/GaN MQWs (InGaIn quantum well: 2.5 nm and GaIn barrier: 13.5 nm) as an active region, and then a 20 nm p-type $\text{Al}_{0.2}\text{Ga}_{0.8}\text{N}$ as a blocking layer. Finally, a 150 nm p-type GaIn is grown. Due to the dielectric mask, the LED growth is limited within the preformed SiO_2 microholes, naturally forming regularly arrayed μ LEDs. By this approach, μ LEDs (including diameter, location, and shape) are fully determined by the SiO_2 microhole masks, where the pitch size and the pitch-to-pitch spacing determine the resolution of the final microdisplay. In our case, the diameter of each μ LED and the edge-to-edge spacing are 20 μm and 25 μm , respectively, leaving enough space for electronic part integration. It is worth highlighting that the size of μ LEDs can be further reduced, leading to a further reduction in the gate-width of a transistor for current driving. A reduced pixel size and pixel-to-pixel distance may be helpful for further enhancing a resolution. By using this direct epitaxial approach, a high resolution with a 3.6 μm pitch size and a 2 μm edge-to-edge spacing have been achieved.^[24,25] This direct epitaxial approach also means that the formation of μ LED arrays does not involve any μ LED mesa etching processes. Please refer to Figure S1a–d (Supporting Information) for our detailed selective growth processes. By means of using

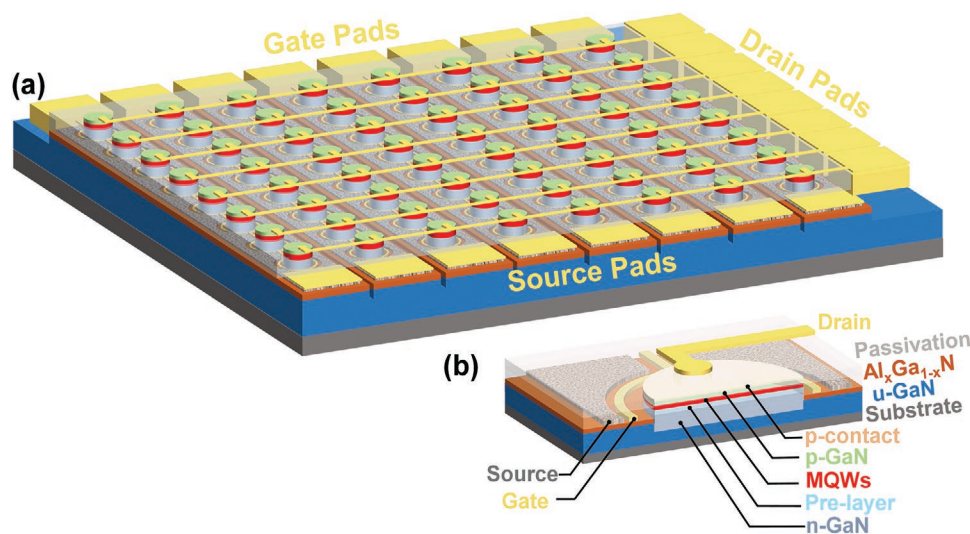


Figure 1. a) 3D layout of our 8×8 μ LED microdisplay; b) schematic of the cross section of a single μ LED, demonstrating each μ LED can be electrically driven by the circular gate of each HEMT surrounding a μ LED.

the selective overgrowth approach on a prepatterned HEMT template, μ LEDs and HEMTs are epitaxially integrated. The next step is due to integrated device fabrication. Figure S1e–l (Supporting Information) provides the schematic of our integrated device fabrication procedure.

Figure 1b illustrates each μ LED which is surrounded by an individual HEMT, where a circular gate in each HEMT controls injection current into each μ LED. Figure 1a indicates that all the circular gates in each column are eventually connected to a gate pad located on one side of the 8×8 μ LED microdisplay, while all the semicircular sources (Ti/Al/Ni/Au metal stacks which undergo rapid thermal annealing (RTA)) represented by grey color in each column are connected to a source pad (Ti/Al/Ti/Au)

on another side. All the p-contacts on top of each μ LED in each row are connected to a drain pad (Ti/Al/Ti/Au). Between two neighboring columns, an isolation trench with a width of $3 \mu\text{m}$ and a depth of 300 nm is formed by etching down to the semi-insulating GaN buffer of the HEMT structure for an insulation purpose by an inductive-coupled plasma (ICP) technique.

3. Results and Discussions

Figure 2a shows the tilted scanning electron microscopy (SEM) image of our single μ LEDs after selective overgrowth and then oxide mask removal.

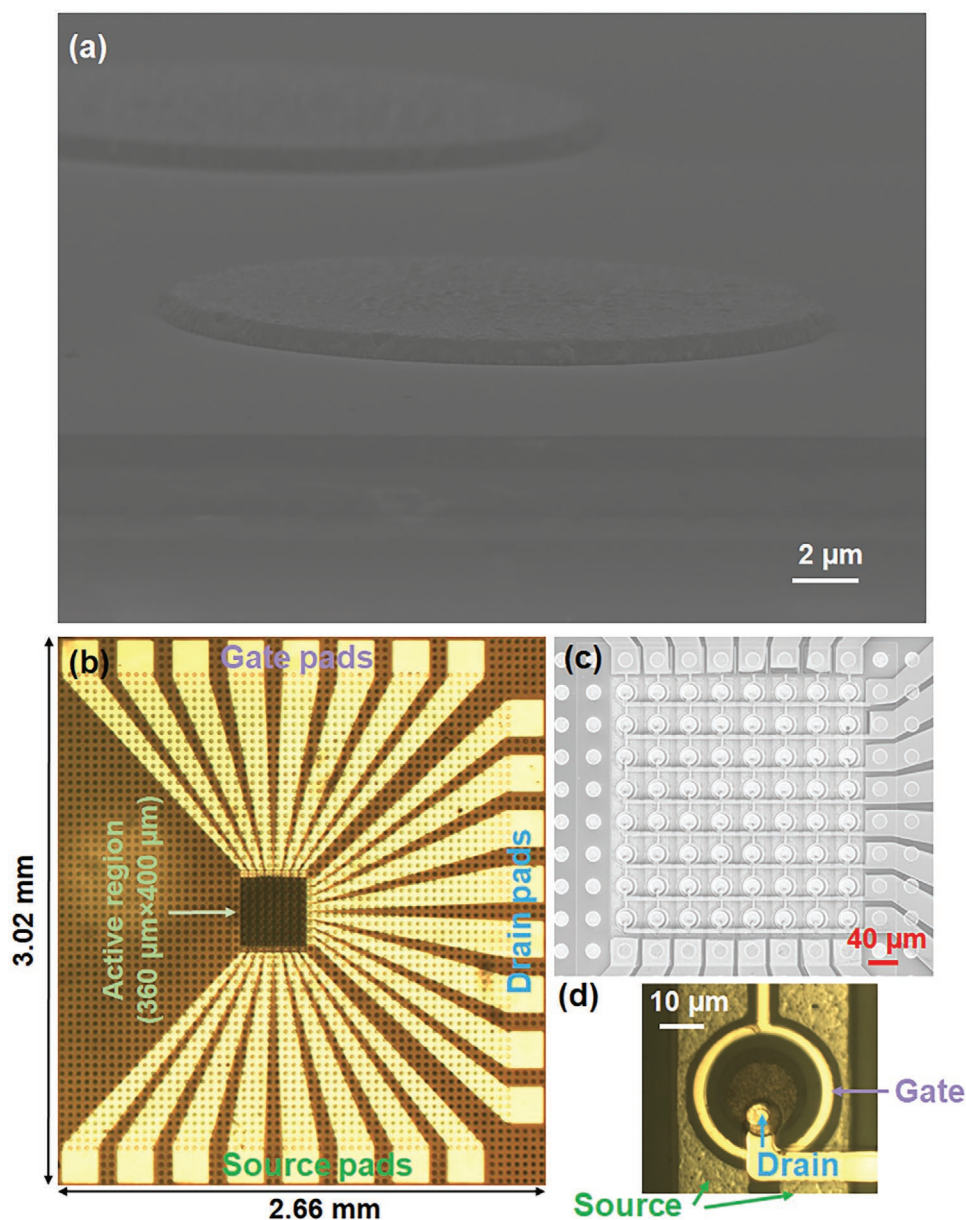


Figure 2. a) Tilted SEM image of our overgrown μ LEDs; b) optical microscopic image of our 8×8 integrated μ LEDs/HEMTs microdisplay; c) SEM image of the screen region of each microdisplay; d) a single μ LED/HEMT integrated unit as a pixel, showing that each $20 \mu\text{m}$ μ LED is surrounded by an individual HEMT (scale bar: $10 \mu\text{m}$).

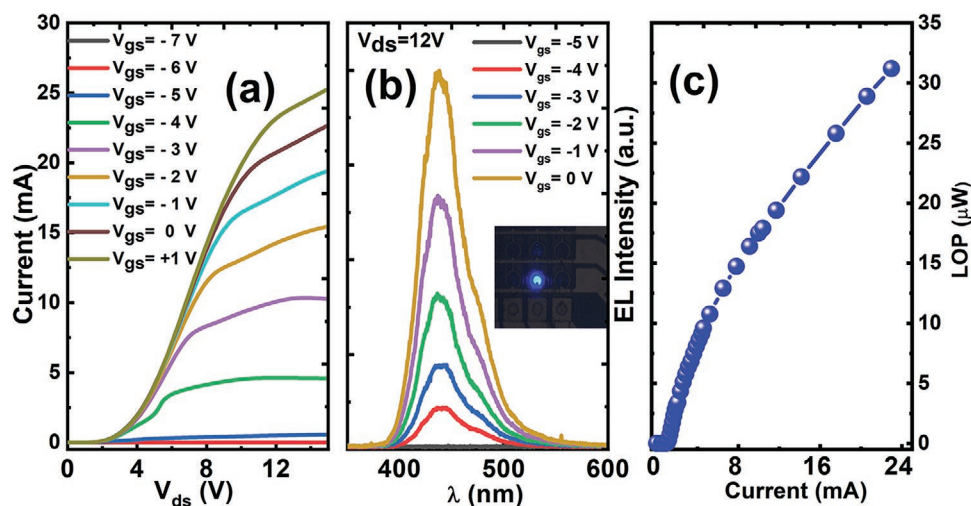


Figure 3. a) Typical I - V characteristics of a single μ LED/HEMT integrated unit; b) typical EL spectra of a single μ LED driven by an individual HEMT as a function of gate bias; Inset: Typical EL image from a single μ LED driven at a gate-source bias $V_{gs} = 0$ V and a drain-source bias $V_{ds} = 12$ V; c) LOP as a function of injection current for a single μ LED/HEMT device.

Figure 2b displays the optical microscopic image of our 8×8 integrated μ LEDs/HEMTs microdisplay, showing $2.66 \text{ mm} \times 3.02 \text{ mm}$ in dimension for each microdisplay chip. The rectangular screen region with a size of $360 \mu\text{m} \times 400 \mu\text{m}$ consists of 8×8 integrated μ LEDs/HEMTs.

Figure 2c shows the SEM image of the screen region of each microdisplay. Each drain pad which connects all the pixels in a same row is deposited on a $2 \mu\text{m}$ SU8-2 passivation layer, while each source pad and each gate pad connecting all the pixels in a same column locate below the passivation layer. Such a design avoids the use of double or triple passivation layers, thus simplifying the fabrication process.

Figure 2d displays a typical single μ LED/HEMT pixel, showing that each $20 \mu\text{m}$ μ LED is surrounded by an individual HEMT. The drain of each μ LED is located on the transparent p-type contact made of Ni/Au alloy which has undergone a thermal annealing process. In each HEMT, the gate length, the gate-to-source distance, and the gate width are $2 \mu\text{m}$, $2 \mu\text{m}$, and $88 \mu\text{m}$, respectively.

Figure 3a shows the typical current-voltage (I - V) characteristics of a single μ LED/HEMT integrated unit, indicating a typical HEMT characteristic. Figure 3b exhibits the typical electroluminescence (EL) spectra of a single μ LED driven by an individual HEMT as a function of gate bias, where inset provides an EL image from a single μ LED driven at a gate-source bias $V_{gs} = 0$ V and a drain-source bias $V_{ds} = 12$ V as an example. Figure 3b shows that the EL intensity of a single μ LED can be modulated by a gate bias from -5 to 0 V. Figure 3c shows the light output power (LOP) of a single μ LED measured as a function of injection current. The emission is collected by an objective lens ($40\times$, 0.75 NA) and then detected by a power meter (Thorlabs PM100D).

Figure 4a shows an equivalent circuit for our 8×8 integrated μ LEDs/HEMTs microdisplay. Gate and source terminals in each column are introduced into G1-G8 and S1-S8, respectively. Drain terminals in each row are introduced into A1-A8. These terminals are eventually wire bonded into a $2.6 \text{ cm} \times 3 \text{ cm}$ PCB

as shown in Figure 4b, where all the source terminals on the PCB are converted into two pins, while the gate terminals and the drain terminals remain separated pins for an easy control purpose.

Figure 4c shows our electrically driving scheme for our 8×8 integrated μ LEDs/HEMTs microdisplay. As mentioned above, the turn-on voltage for a gate and the operation voltage for a drain are different from that used for a conventional seven-segment display (typically for driving standard LEDs). As a result, a standard Max7221 chip which is commercially available does not match our integrated microdisplay and thus cannot be adopted here.

To address this issue, a different design is required. In our design, source terminals are directly introduced to a $+5 \text{ V}$ power supply (provided by Keithley 2400). In this case, we do not need to further convert a positive 0 to $+5 \text{ V}$ SEG signal into a negative voltage which is used to switch on/off a HEMT. Since the source terminals are at $+5 \text{ V}$, the voltage drop from the gates to the sources can be tuned from -5 to 0 V , which is good enough to use the gate to switch on/off a HEMT. To bypass the SEG current, $20 \text{ k}\Omega$ resistors are used between the SEG signals and ground prior to being introduced to the gate terminals.

For the drain terminals, an analog circuit as shown in Figure 4c is used to boost the DIG signal to a higher voltage level ($>10 \text{ V}$). To achieve such a function, the circuit suggested in Max 7221's application note^[28] has been modified, where two MOSFETs have been adopted, namely, Q2 which is IRF9520 (p-channel) and Q3 which is IRF510 (n-channel). The drain terminals of Q2 are connected to the drain terminals. A CPU controlled Arduino board is used to provide clock (CLK), data (DIN), chip-selection (CS), V_{cc} ($+5 \text{ V}$), and GND signal to the Max 7221 chip. Our test setup and driving PCB are displayed in Figure 4d.

Finally, our 8×8 integrated μ LEDs/HEMTs microdisplay has been demonstrated through a short video showing "I ♥ Sheffield" which can be found in the Supporting

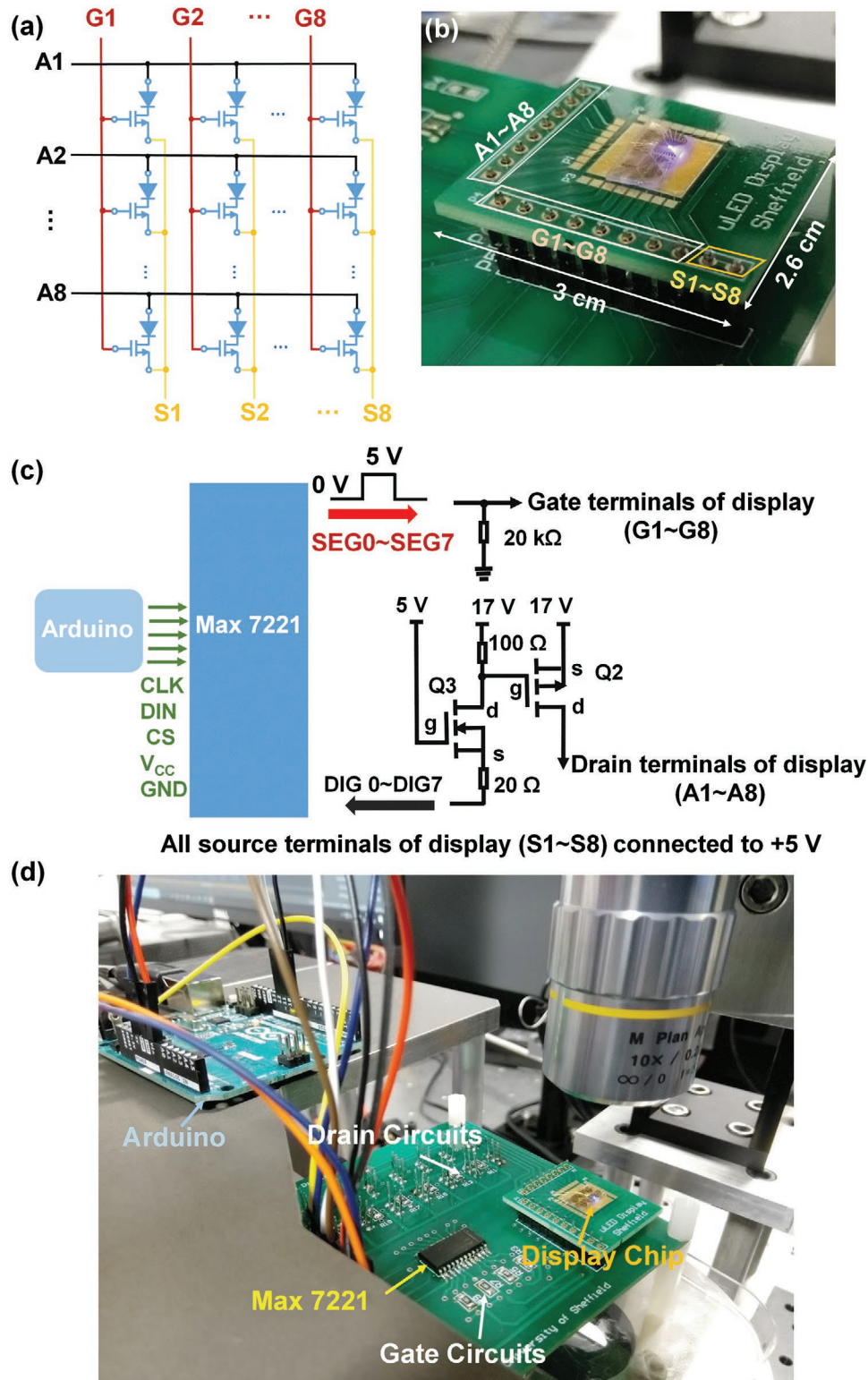


Figure 4. a) Equivalent circuit for our 8×8 integrated μ LEDs/HEMTs microdisplay; b) Our PCB where all the gate terminals, source terminals, and drain terminals are wire-bonded; c) our electrically driving scheme for our 8×8 integrated μ LEDs/HEMTs microdisplay; d) photo of our test setup and driving PCB.

Information. The video has been recorded via a CCD camera mounted on a light collection system consisting of a 10 \times objective lens and a NAVITA 12 \times Zoom Lens System as shown in Figure 5a.

Figure 5b shows the images which are captured from the short video for a demo purpose. The delay between each letter in the video is 1000 ms, which can be changed through the

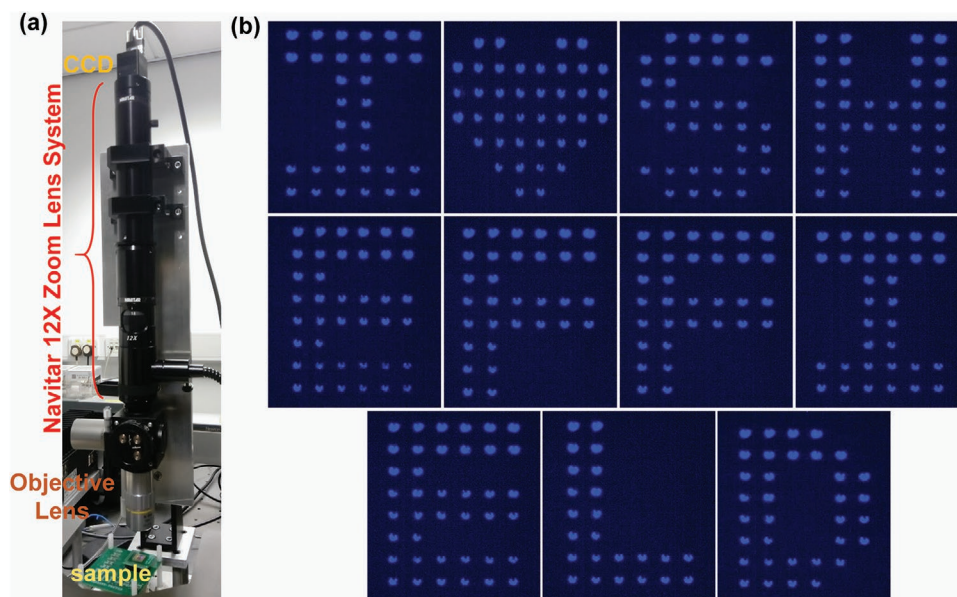


Figure 5. a) Optical image of our light collection system for recording a short video using our 8×8 microdisplay; b) images (“I ♥ Sheffield”) which are captured from the short video for a demo purpose.

code in Arduino. By means of changing the duty cycle of the gate pulse, the EL intensity of individual μ LED pixel can be modified using a pulse-width-modulation (PWM) scheme^[29] to obtain a high-contrast-ratio display.

It is worth highlighting that such each μ LED/HEMT integrated unit can be controlled by both gate voltage and drain voltage. As a consequence, such an integrated unit can also play a visible light communication (VLC) role in addition to its microdisplaying function.^[30–32] Except for this dual-functionality application, such an integrated device can also be adopted for much broader fields, such as display and flexible biomedical applications,^[33,34] quantum dot color-converting layers for a full color display, etc.^[35,36]

4. Conclusion

In conclusion, we have developed an epitaxial approach to monolithically integrate μ LEDs and HEMTs on a single chip by means of using a selective overgrowth method on a pre-defined HEMT template featuring SiO_2 microhole masks. Our approach has eliminated all the fundamental issues which cannot be overcome in either “pick-and-place” approach or “flip-chip bonding” technology. Finally, we have translated the proposed epitaxial integration concept into a prototype, demonstrating an 8×8 microLED microdisplay, where each μ LED is electrically driven by an individual HEMT which surrounds its respective μ LED via the gate bias of the HEMT.

Supporting Information

Supporting Information is available from the Wiley Online Library or from the author.

Acknowledgements

Financial support is acknowledged from the Engineering and Physical Sciences Research Council (EPSRC), UK via EP/P006973/1, EP/M015181/1, and EP/P006361/1. The authors would like to acknowledge Dr. Yuan Gao at School of Microelectronics, Southern University of Science and Technology, for a useful discussion about driving circuit design.

Conflict of Interest

The authors declare no conflict of interest.

Author Contributions

T.W. conceived the idea and organized the project. T.W. and Y.C. prepared the manuscript. Y.C. designed a device layout, patterned HEMT templates, performed device fabrication, designed the analog control circuits and led the circuit test. C.Z. and P.F. prepared HEMT templates, performed selective overgrowth of μ LEDs and material characterization. W.Z. contributed to PCB design and circuit test. S.J. contributed to PCB design and circuit test on an initial stage.

Data Availability Statement

The data that support the findings of this study are available from the corresponding author upon reasonable request.

Keywords

GaN, HEMTs, microdisplay, microLEDs, selective overgrowth

Received: February 22, 2021

Revised: March 18, 2021

Published online:

- [1] Y. Huang, E. L. Hsiang, M. Y. Deng, S. T. Wu, *Light Sci. Appl.* **2020**, 9, 1.
- [2] Y. H. Lee, T. Zhan, S. T. Wu, *Virtual Real. Intell. Hardw.* **2019**, 1, 10.
- [3] Z. Y. Fan, J. Y. Lin, H. X. Jiang, *J. Phys. D: Appl. Phys.* **2008**, 41, 094001.
- [4] M. Y. Soh, W. X. Ng, T. H. Teo, S. L. Selvaraj, L. Peng, D. Disney, Q. Zou, K. S. Yeo, *IEEE Trans. Electron Devices* **2019**, 66, 4221.
- [5] H. X. Jiang, S. X. Jin, J. Li, J. Shakya, J. Y. Lin, *Appl. Phys. Lett.* **2001**, 78, 1303.
- [6] T. Wu, C. W. Sher, Y. Lin, C. F. Lee, S. Liang, Y. Lu, S. W. H. Chen, W. Guo, H. C. Kuo, Z. Chen, *Appl. Sci.* **2018**, 8, 1557.
- [7] C. W. Jeon, H. W. Choi, M. D. Dawson, *Phys. Status Solidi A* **2003**, 200, 79.
- [8] J. J. McKendry, D. Massoubre, S. Zhang, B. R. Rae, R. P. Green, E. Gu, R. K. Henderson, A. E. Kelly, M. D. Dawson, *J. Light Technol.* **2011**, 30, 61.
- [9] C. J. Chen, H. C. Chen, J. H. Liao, C. J. Yu, M. C. Wu, *IEEE J. Quantum Electron.* **2019**, 55, 1.
- [10] X. Zhang, P. Li, X. Zou, J. Jiang, S. H. Yuen, C. W. Tang, K. M. Lau, *IEEE Photonics Technol. Lett.* **2019**, 31, 865.
- [11] L. Zhang, F. Ou, W. C. Chong, Y. Chen, Q. Li, *J. Soc. Inf. Disp.* **2018**, 26, 137.
- [12] F. Templier, *J. Soc. Inf. Disp.* **2016**, 24, 669.
- [13] V. W. Lee, N. Twu, I. Kymissis, *J. Inf. Disp.* **2016**, 32, 16.
- [14] B. Corbett, R. Loi, W. Zhou, D. Liu, Z. Ma, *Prog. Quantum Electron.* **2017**, 52, 1.
- [15] R. S. Cok, M. Meitl, R. Rotzoll, G. Melnik, A. Fecioru, A. J. Trindade, B. Raymond, S. Bonafede, D. Gomez, T. Moore, C. Prevatte, *J. Soc. Inf. Disp.* **2017**, 25, 589.
- [16] E. H. Virey, N. Baron, *SID Int. Symp. Dig. Tech.* **2018**, 49, 593.
- [17] J. G. Um, D. Y. Jeong, Y. Jung, J. K. Moon, Y. H. Jung, S. Kim, S. H. Kim, J. S. Lee, J. Jang, *Adv. Electron. Mater.* **2019**, 5, 1800617.
- [18] P. Tian, J. J. McKendry, Z. Gong, B. Guilhabert, I. M. Watson, E. Gu, Z. Chen, G. Zhang, M. D. Dawson, *Appl. Phys. Lett.* **2012**, 101, 231110.
- [19] F. Olivier, A. Daami, C. Licitra, F. Templier, *Appl. Phys. Lett.* **2017**, 111, 022104.
- [20] F. Olivier, S. Tirano, L. Dupré, B. Aventurier, C. Largeron, F. Templier, *J. Lumin.* **2017**, 191, 112.
- [21] J. Kou, C. C. Shen, H. Shao, J. Che, X. Hou, C. Chu, K. Tian, Y. Zhang, Z. H. Zhang, H. C. Kuo, *Opt. Express* **2019**, 27, A643.
- [22] J. M. Smith, R. Ley, M. S. Wong, Y. H. Baek, J. H. Kang, C. H. Kim, M. J. Gordon, S. Nakamura, J. S. Speck, S. P. DenBaars, *Appl. Phys. Lett.* **2020**, 116, 071102.
- [23] M. S. Wong, D. Hwang, A. I. Alhassan, C. Lee, R. Ley, S. Nakamura, S. P. DenBaars, *Opt. Express* **2018**, 26, 21324.
- [24] J. Bai, Y. Cai, P. Feng, P. Fletcher, X. Zhao, C. Zhu, T. Wang, *ACS Photonics* **2020**, 7, 411.
- [25] J. Bai, Y. Cai, P. Feng, P. Fletcher, C. Zhu, Y. Tian, T. Wang, *ACS Nano* **2020**, 14, 6906.
- [26] Y. Cai, J. I. H. Haggard, C. Zhu, P. Feng, B. Jie, T. Wang, *ACS Appl. Electron. Mater.* **2021**, 3, 445.
- [27] S. Jiang, Y. Cai, P. Feng, S. Shen, X. Zhao, P. Fletcher, V. Esendag, K. B. Lee, T. Wang, *ACS Appl. Mater. Interfaces* **2020**, 12, 12949.
- [28] Application Note 1196, Using the Max7219/7221 to drive higher voltage or current, Homepage, <https://www.maximintegrated.com/en/design/technical-documents/app-notes/1/1196.html> (accessed: September 2002).
- [29] Y. Cai, X. Zou, C. Liu, K. M. Lau, *IEEE Electron Device Lett.* **2018**, 10, 1.
- [30] X. Liu, R. Lin, H. Chen, S. Zhang, Z. Qian, G. Zhou, X. Chen, X. Zhou, L. Zheng, R. Liu, P. Tian, *ACS Photonics* **2019**, 6, 3186.
- [31] X. Li, L. Wu, Z. Liu, B. Hussain, W. C. Chong, K. M. Lau, C. P. Yue, *J. Light Technol.* **2016**, 34, 3449.
- [32] D. Peng, K. Zhang, Z. Liu, *IEEE J. Electron Devices Soc.* **2016**, 5, 90.
- [33] H. E. Lee, J. Choi, S. H. Lee, M. Jeong, J. H. Shin, D. J. Joe, D. Kim, C. W. Kim, J. H. Park, J. H. Lee, D. Kim, *Adv. Mater.* **2018**, 30, 1800649.
- [34] H. E. Lee, J. H. Shin, J. H. Park, S. K. Hong, S. H. Park, S. H. Lee, J. H. Lee, I. S. Kang, K. J. Lee, *Adv. Funct. Mater.* **2019**, 29, 1808075.
- [35] H. Y. Lin, C. W. Sher, D. H. Hsieh, X. Y. Chen, H. M. P. Chen, T. M. Chen, K. M. Lau, C. H. Chen, C. C. Lin, H. C. Kuo, *Photonics Res.* **2017**, 5, 411.
- [36] Z. Liu, C. H. Lin, B. R. Hyun, C. W. Sher, Z. Lv, B. Luo, F. Jiang, T. Wu, C. H. Ho, H. C. Kuo, J. H. He, *Light: Sci. Appl.* **2020**, 9, 1.